DI Dr. Jennifer Simonjan

NANOSCALE SENSOR NETWORKS

Nanotechnology in Sensors and Communications

FINAL REPORT

Research stay at the Georgia Institute of Technology
from 15 January 2020 until 2 August 2020.

Alpen-Adria-Universität Klagenfurt

Sup.: Univ.–Prof. Dr. Bernhard Rinner
Pervasive Computing Group
Institute of Networked and Embedded Systems

Georgia Institute of Technology

Sup.: Univ.–Prof. Dr. Ian F. Akyildiz
Broadband Wireless Networking Lab
School of Electrical and Computer Engineering

August 2020

Acknowledgements

Prior to the research report, I want to acknowledge the people and funding agencies who have enabled my research stay abroad. First, I would like to express my sincere gratitude to Prof. Bernhard Rinner and Prof. Ian F. Akyildiz for their remarkable support throughout the entire research stay. Without their help and support I would not have been able to perform this research stay. Sincere gratitude also goes to both universities, the Alpen-Adria Universität Klagenfurt (AAU) and the Georgia Institute of Technology (Georgia Tech) for granting and supporting my research and to all my lab members and colleagues. I am thankful for the opportunity to collaborate with both professors, as their expertise has greatly influenced and shaped my personal academic career and research agenda.
A very particular gratitude goes to the funding agencies enabling my research stay abroad. I was supported through scholarships from the Austrian Marshall Plan Foundation and the Federation of Austrian Industries (Industriellenvereinigung Kärnten) and the Austrian Economic Chambers (Wirtschaftskammer Kärnten).
Furthermore, I am deeply thankful for receiving so much support from my family and friends. They did not only encourage me to pursue research abroad, but were also my major emotional supporters during the difficult COVID-19 times. A big thanks also goes to my roommates, who were of great emotional support and with whom I had a great time even during the Coronavirus lock-down. Thanks for all your help and great support.

Abstract

Nanotechnology is enabling the development of a new generation of devices which are able to sense, process and communicate, while being in the scale of tens to hundreds of cubic nanometers. Such small, imperceptible devices enhance not only current applications but enable entirely new paradigms especially for in-body environments. This report introduces a localization and tracking concept for measurements of nanosensors floating through the human bloodstream. Besides the nanoscale sensors, the proposed systems also comprises macroscale anchor nodes attached to the skin of the monitored person. To realize autonomous localization and resource-efficient wireless communication between sensors and anchors, we propose to rely on inertial positioning and sub-terahertz backscattering communication as major building blocks. Our proposed system is a first step towards early disease detection as it aims at localizing body regions which show anomalies. Simulations have been conducted to enable a systematical evaluation on the feasibility of the approach.

Contents

1 Introduction

Novel nanomaterials like graphene and its derivatives have made it possible to fabricate tiny sensors, i.e., (bio)nanosensors, which are capable of detecting the smallest changes in physical variables, such as pressure, vibrations, temperature and concentrations in chemical and biological molecules [1]. Besides the sensor itself, additional components of a nanosensor comprise a memory, a processor, a transceiver, an antenna and a battery. The main components of a nanosensor can thus be summarized as follows [2]:

- **Nano-sensor** represents the sensing unit. Examples include all types of sensors such as photodetectors, ultrasonic sensors and chemical sensors to build e.g., nano-cameras [3], nano-phones and nano-accelerometers, respectively.
- **Nano-memories** store sensed or received information. Current technology enables single-atom nano-memories [4], whose dimensions define the amount of stored information.
- **Nano-processors** process sensed or received information. Nanofabrication already allows to create electronic components such as transistors or logic gates from nanomaterials, enabling the development of nano-processors [5].
- **Nano-transceivers and -antennas** establish data communication (e.g., Terahertz-band communication [6]) between nanosensors and enable the transfer of sensor data and eventually the deployment of a nanosensor network.
- **Nano-batteries** [7] in combination with nanoscale energy harvesting systems [8] provide the power-supply for nanosensors. The device size imposes limits for the amount of the energy harvested and stored.

All components are built upon so-called nanomaterials, which form the major enabling technology for nanosensors as they allow to develop electronic circuitry and sensing components on a nanoscale. By definition, nanomaterials have at least one dimension between 1 nm and 100 nm [9].
Naturally, the size and arrangement of the individual components directly influence the capabilities and properties of the nanosensor including processing power, memory capacity, energy capacity and communication abilities. Further, the area of the nanosensor determines the total number of sensing units which affects the detection capabilities (e.g., resolution of a nano-camera depends on the number of photodetectors).
Such invisibly small sensors enable to see and sense molecules which are too small to be seen otherwise. One reason for late detections of diseases like cancer, is that current sensing technology can only detect them once they are manifested in the

organs and have a sufficient high molecule concentration. Nanosensors are however capable of detecting much lower concentrations and enable thus to detect diseases at a much earlier development stage [10, 11]. As an example, glucose molecules and cancer cells have sizes in the range of a few nano- to micrometers. The only possibility to detect such small molecules is to have sensors with extraordinary high sensitivity while being in the size of the biomolecules themselves. Nanosensors are already in the development and will revolutionize in-body applications in the near future.

To be able to detect diseased cells in the human body, hundreds or thousands of nanosensors are foreseen to float through the cardiovascular system in order to check for anomalies. Whenever such an anomaly occurs the sensors should detect and report it to the outside world. A major concern in this field is thus to localize the body regions at which anomalies have been detected. Such a localization system is inherently very challenging due to the highly dynamic environment, the extremely constrained resources of the nanosensors and the wireless communication through human tissue.

In this work, we propose a system architecture to localize and track nanosensor measurements used for in-body health monitoring applications. Figure 1 depicts an overview of the foreseen system which comprises anchor nodes and nanosensors. Anchor nodes are of macroscale size and are attached to the skin of the monitored person while the sensors are of nanoscale size and float through the bloodstream. Instead of providing up-to-date location information of the highly dynamic sensors themselves, we propose to equip their sensor readings with information about the locations at which they were performed. Relying on highly mobile sensors without the possibility of influencing them much, we require the sensors to track their locations themselves. Thus, we propose to equip the sensors with Inertial Measurement Units (IMUs) composed of nanoscale accelerometers and gyroscopes. Having access to IMU readings, sensors are able to exploit inertial positioning and can thus add location information to their actual sensor readings (i.e., pressure, temperature, vibration, molecule concentration).

Furthermore, sensors need to communicate their findings to the anchors in order to make them accessible to the operator, i.e., the physician. Graphene-based nanoantennas have been shown to efficiently operate in the sub-terahertz band (0.1-10 THz) [12], which in turn enables short distance communication in human tissue [13]. Such communication between the nanosensors thus enables the realization Wireless Nanoscale Sensor Networks (WNSNs). To ensure resource-efficiency, we propose to rely on THz backscattering communication between sensors and anchors. The main advantage of backscattering communication is, that the passive communication partners (i.e., the sensors) do not need to actively generate radio-frequency (RF) signals but harvest energy from the signals of the active communication partners (i.e., the anchors) instead.

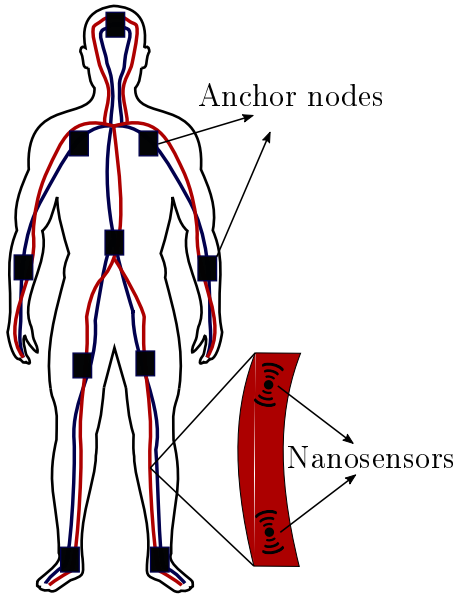

Figure 1: Contour of a human body including the major vessels. Anchor nodes are attached to the skin and nanosensors are floating inside the vessels.

Up until now, there is only very little research on the localization of in-body nanosensors and even less meaningful evaluation approaches. The main contributions of our work are a novel, realistic system model for localization and tracking of in-body nanosensor measurements and a systematical evaluation of the proposed approach. As the localization performance relies on the placement of the anchors and on the THz backscattering communication, we provide two kinds of evaluation results: i.) channel model, path loss and capacity of THz backscattering communication channel in human tissue and ii.) suggestions for the placement of anchors considering the nanosensor movement and the limited resources.
The remainder of this report is organized as follows. Section 2 introduces the related work in in-body localization, in THz backscattering localization and in localization based on inertial positioning. The building blocks of our proposed system including the nanosensors, the anchor nodes and the wireless communication technology are explained in Section 3. Section 4 introduces our localization concept and Section 5 discusses the feasibility of the concept by evaluating the system. We conclude the report and outline future work in Section 6 and discuss our dissemination strategies in Section 7.

2 Related work

The problem of autonomously localizing wireless sensor nodes or mobile robots has been well studied in the past decades, resulting in a large variety of localization algorithms for all kinds of networks [14, 15, 16]. Wireless sensor network localization approaches often exploit signal strength measurements or hop counts of messages while mobile robot localization often relies on inertial positioning. The related work first discusses standard localization methods in order to get a good overview and background on the topic. Afterwards, we specifically focus on the current state-of-the-art in in-body nanosensor localization and THz backscattering localization. Furthermore, we briefly discuss inertial positioning methods (also referred to as dead reckoning) in mobile networks.

2.1 Wireless sensor network localization

The problem of autonomously localizing sensor nodes within a network has been well studied in the past decades, resulting in a large variety of self-calibration algorithms for sensor networks, specifically for traditional wireless sensor networks (WSNs). Wireless sensor network localization approaches are typically classified into range-based and range-free methods. Range-based methods rely on distance and angle estimations between the sensor nodes, while range-free methods exploit radio connectivity to infer the locations of the nodes [15, 17, 18, 19]. Well known examples for range-free calibration schemes include the Distance Vector (DV) hop and the Approximate Point-In-Triangulation (APIT) scheme. DV hop estimates the range between nodes and basestations (which have known positions) using the hop count of messages broadcasted by the basestations [20]. Through this mechanism, all nodes determine the shortest distance, in hops, to every basestation. To convert hop count into physical distance, each basestation obtains location and hop count information for all other basestations in the network. Compared to DV hop, APIT requires a heterogeneous network of sensing devices of which a small percentage are equipped with GPS, referred to as anchors. Using beacons from these anchors, APIT employs an area-based approach to perform location estimation by isolating the environment into triangular regions between anchors [17]. The area in which a node can potentially reside is then constrained by the presence of the node in- or outside of these triangular regions. It is questionable if it will be possible to deploy anchors with GPS modules in nanosensor networks, which leads us to aim for non-GPS-based solutions. The disadvantage of localization approaches exploiting the hop count of messages is the accuracy which solely relies on the network connectivity quality. To enhance the accuracy, hop count based approaches rely on a dense and uniform network structure, which might or might not be feasible for nanosensor networks, depending on the application. Additionally, hop counting lo-

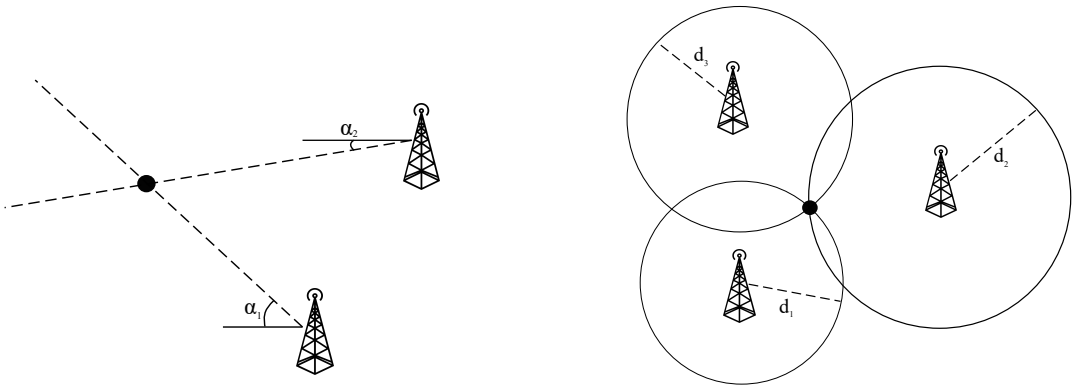

Figure 2: Geometric localization based on (a) angle-of-arrival (AOA) measurements and on (b) distance related measurements. The black circle depicts the sensor node. AOA measurements are used for triangulation, which determines the location of the sensor by forming triangles. Distance measurements are on the other hand used to determine the unknown location through multi-lateration.

calization schemes typically introduce a high message overhead in the network and are not suited for dynamic networks with mobile nodes.

Range-based localization approaches on the other hand exploit distance and angle measurements to estimate positions of others. In general they can be classified into the following three categories [21, 22]: i) angle-of-arrival (AOA) measurements, ii) distance-based measurements and iii) Received Signal Strength (RSS) profiling. AOA measurements make use of the beamforming pattern of antennas to determine the angle between nodes [18]. To do so, sensor nodes need dedicated antenna arrays leading to a strong hardware-constraint which might not be suitable for nanosensors [23]. Distance related measurements rely on propagation time based measurements to determine the distance between nodes [24] and RSS profiling methods construct a map of the signal strength behavior in the coverage area [19]. Figure 2 depicts the geometric calculations used for AOA- and distance-based calibration. The process of triangulation is shown in Figure 2 (a). Triangulation relies on AOA measurements to form triangles which are then used to determine the unknown position. Figure 2 (b) depicts the process of multi-lateration, which relies on circles to find the unknown position. The radii of the circles are the distances measured to certain anchor points or basestations. Distances can easily be determined based either on time of arrival measurements, if the propagation speed of the wave is known, or on RSS measurements. A comprehensive survey of state-of-the-art WSN self-calibration methods can be found in [25].

2.2 In-body localization

To the best of our knowledge, as well as according to [26], there are only very few attempts towards the localization of in-body nanosensors operating in the THz band. Furthermore, all of them focus on localizing the nanosensors themselves rather than anomalies in the body, which is realistically difficult to achieve due to their high mobility.

One approach, which has been proposed in [27], introduces two hop-counting based localization algorithms. Their first technique exploits flooding in order to estimate distances between nanonodes from the number of hops. Since there is a huge message overhead, the second technique proposes to establish clusters first. Only cluster heads communicate with each other in order to localize certain nodes. The simulation model assumes a 100 cm^2 square area with uniformly distributed nodes and communication ranges of $1-2$ cm providing thus very limited evaluation results for the in-body scenario.

Another method proposes a pulse-based distance accumulation (PBDA) localization algorithm for WNSNs which is used to estimate the distance between anchors and clustered nodes [23]. The simulated system model considers a 2D square area with randomly deployed nodes. First, nodes run a classification algorithm based on the flooding mechanism, which classifies all nodes into corner, border or center nodes. Afterwards, a clustering algorithm establishes clusters and identifies cluster heads. Finally, flooding packets are forwarded through cluster heads in order to calculate the distance between corner nodes based on hops. The algorithm adopts femtosecond-long pulse for terahertz band communication based on on-off keying (OOK) modulation. Similar to [27], the considered simulation model can barely evaluate an in-body scenario.

Shree et al. [28] have introduced a further approach in which they utilize the MUltiple SIgnal Classification (MUSIC) [29] algorithm in order to systematically study the Direction of Arrival (DOA) estimation for nanosensor networks. The study was done for different energy levels, distances, pulse shapes and frequencies. In the simulations the authors consider the terahertz channel as standard air medium. Their investigations showed that the error can be reduced by selecting lower order and higher frequency pulses for transmission. A successful estimation of the angle of arrival could enable localization in nanosensor networks, however, sensor would need dedicated antenna arrays. Further, reliable DOA estimation is difficult in in-body scenarios in which sensors are highly mobile, floating inside vessels while frequently changing their orientation.

Summarized, none of the above mentioned localization approaches provide dedicated evaluation results for the in-body environment. Furthermore, most of the simulations are rather general and do not consider the very specific energy and communication constraints of nanosensors.

2.3 THz backscattering localization

One promising direction towards obtaining accurate distance measurements, while at the same time maintaining low energy consumption, is to exploit backscattered signals for localization purposes [26]. The feasibility and promising accuracy of such an approach has been demonstrated on the macro-level in [30] and [31]. El-Absi et al.[30] exploit backscattered THz signals to extract the round-trip time-of-flight (RToF) between nodes and anchors in order to determine the distance. Multiple RToF readings from different anchors are then used to estimate the location of the node utilizing the linear least square algorithm. There are two main advantages of backscattering: First, the nodes do not need to actively generate signals, but only to modulate and reflect received ones. Second, there is no clock drift which could affect the distance estimates since the RToF is determined only by the reader, which is equipped with a high-accuracy clock [26]. However, the network in [30] was assumed to be of static nature and the solution does thus not fit an in-body scenario with highly dynamic sensors.
Lemic et al. [31] have proposed a method to localize software-defined metamaterial (SDM) elements by utilizing THz backscattering communication for frequencies of 300 GHz to 10 THz. The localization relies on trilateration by exploiting distance estimates from RToF measurements between nanonodes and controllers. Through simulations, the authors demonstrate a sub-millimeter accuracy of the localization as well as a high availability and low energy consumption of the approach.
Even though many of the next-generation networks are expected to exploit THz communications to provide accurate locations [32], research on localization algorithms for nanonetworks in the in-body environment is still lacking.

2.4 Localization based on inertial positioning

Inertial positioning, also known as dead reckoning, refers to the process of estimating a node's current position by using its previous position and an estimate about its traveled distance and direction which are recorded by the built-in IMU. IMUs utilize a combination of accelerometers, gyroscopes and sometimes magnetometers to measure the acceleration and rotation of the device they are integrated in. They are often incorporated into Inertial Navigation Systems (INSs) which exploit the IMU measurements to determine the angular rate, the linear velocity and the position of a device relative to a global reference system. Figure 3 depicts the process of inertial positioning. Upon movement of the mobile node, it accumulates its previous position with the recorded angle and traveled distance.
The major advantage of inertial positioning is that it does not rely on external information enabling a fully autonomous navigation. In general, inertial positioning is very accurate over short periods with high update frequency. However, the accuracy

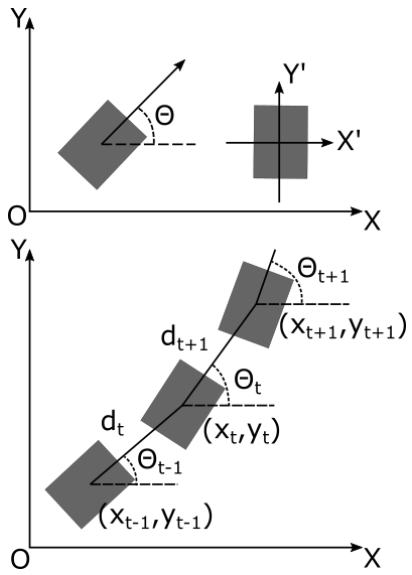

Figure 3: Process of inertial positioning. Upon movement, the mobile node accumulates its previous position with the recorded angle and traveled distance.

of the process is significantly affected by accumulation of noise and drift errors from accelerometers and gyroscopes. Therefore, IMU measurements are often fused with other positioning technologies [33].

In the field of robotics, a variety of IMU-based localization systems have been developed in order to localize and track mobile robots during their missions [33, 16, 34]. Li et al. [16] present i.e., a deep learning approach to localize a mobile robot using a 2D laser and an IMU. For that purpose, a novel Recurrent Convolutional Neural Network (RCNN) architecture is developed to fuse the laser and IMU data for pose estimation. Another method which also aims at accurately locating mobile robots based on sensor fusion has been proposed by Marquez et al. [33]. The approach fuses acceleration from an IMU and the 2-D coordinates received from the Ultra-Wideband (UWB) anchors together in a Kalman filter to achieve an accurate location estimation. A further approach for Kalman filter based localization was introduced by Malyavej et al. [34]. The authors propose to localize mobile robots by exploiting sensor fusion of Received Signal Strength Indicator (RSSI) measurements from a WiFi network and IMU measurements. The proposed fusion scheme is based on the extended Kalman filter (EKF).

In general, inertial positioning approaches are expected to be well suited for in-body nanosensor applications since they operate in a fully autonomous manner and do not require any external information.

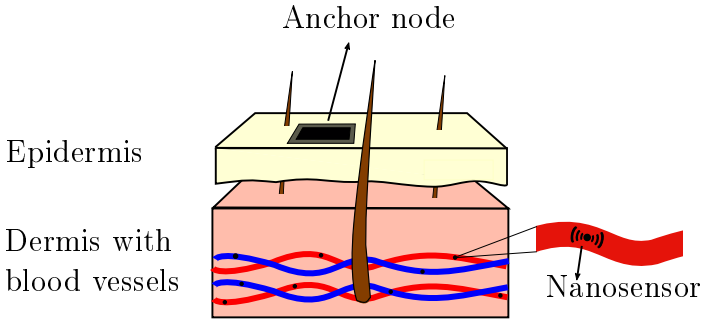

Figure 4: Simplified model of the skin layers, including the epidermis and the dermis with the blood vessels. The nanosensors are floating in the vessels while the anchors are attached to the skin.

3 System model building blocks

Our proposed system is comprised of two kinds of devices, i.e., the nanosensors which are floating inside the human bloodstream and the anchor nodes which are attached to the skin. The anchors are larger in scale and more powerful than the nanosensors. Their main task is to collect sensing and location information from the sensors as they float by. Furthermore, anchors provide radio frequency (RF) signals which are exploited by the sensors to communicate via THz backscattering communication. The nanosensors are tiny sensing devices built upon nanomaterials (i.e., graphene) which are injected into the human bloodstream in order to monitor certain health parameters [35, 36]. Figure 4 depicts an overview of our system model. We assume a simplified model of the skin layers including the epidermis and the dermis, which in turn includes the blood vessels with the floating sensors. Anchor nodes are attached to the skin, i.e., the epidermis.

3.1 Anchor nodes

Anchors are attached across the whole body to the skin of the human who is being monitored. Specifically, the anchors should be attached to regions of the body where the skin and fat layers are thin, i.e., volar forearm, scalp, dorsum of the hand or anterolateral thigh. The anchors are the active components of the backscattering communication system, and serve as basestations and gateways to enable access to the measurements of the nanosensors. Anchors constantly transmit RF signals which are used by the sensors for the backscattering communication. Whenever a sensor is sufficiently close to an anchor and receives its RF signal, it harvests energy from the signal, modulates it to pack its data into the signal and reflects it back to the anchor.

Communication among anchors or between anchors and a sink node (i.e., computer) can be achieved via a standard networking technology such as IEEE 802.11 or 802.15. Our localization concept foresees anchors to maintain tables in which they collect all the received information of the sensors. These tables are periodically sent to a sink computer, where they are merged in order to keep an updated view of the sensors and their measurements. Anchors are synchronized in time to be able to timestamp received packets, while sensors do not need any synchronization.

3.2 Nanosensors

Nanosensors are nanoscale devices which are able to detect, (pre-)process and transfer sensed data. Thus, they are comprised of a sensing, communication and processing unit. Depending on the physical parameter to be monitored, the sensing unit requires a certain type of sensor such as pressure sensors [37], temperature sensors [38], mechanical sensors [39] or optical sensors [3]. Since the nanosensors should provide sensor readings along with location information, they are further equipped with IMUs. IMUs typically comprise an accelerometer and a gyroscope to measure velocity and rotation, respectively. While nanoscale IMUs have not been developed and tested yet, nanoscale accelerometers as well as gyroscopes have already been proposed by the nanotechnology community within recent years [40, 41, 42, 43]. Incorporating them into the nanosensors will allow them for inertial positioning methods similar to those used in mobile robot applications. As already mentioned, communication between nanosensors and anchors relies on backscattering with the sensors being the passive communication partners. Thus, sensors do not need to be equipped with an active RF component. However, they need an energy harvester, a receiver and a modulator in order to exploit and modulate the received signal before reflecting it back to the anchor. Similar to standard sensors, nanosensors also require a memory and a battery unit.

3.3 Wireless communication

The material most commonly associated with nanoantennas at this time is graphene, which is a flat monolayer of carbon atoms tightly packed into a two-dimensional honey-comb lattice [12]. Graphene antennas can efficiently operate at terahertz band frequencies (0.1-10 THz) [44, 12, 45]. With their very small form factor of just tens of nanometers in width and a few micrometers in length, they can easily be integrated into future nanosensors.

These tiny transceivers are however not able to generate carrier signals, which requires to use carrier-less pulse-based communication schemes [45, 28]. Up to now, there are several works which discuss pulse-based modulations schemes suitable for WNSNs [45, 46, 47, 48]. One of the first approaches proposes Time-Spread On-

Off Keying (TS-OOK) and was introduced by Jornet et al. [45]. TS-OOK exploits pulses which are 100 fs long and enforces that the separation between pulses is much longer than the duration of the pulse. The scheme is based on conventional OOK and works thus as follows: A logical "1" is transmitted by a pulse of 100 fs length and a logical "0" is transmitted as silence [45]. This modulation scheme is compatible with very low energy applications and does not require tight synchronization between all nanosensors.
The maximum distance for successful communication between sender and receiver depends on the THz channel. The main issue in THz band communication is the very high path loss due to the molecular absorption loss [49, 50]. Molecular absorption loss is caused by the fact that some molecules in the medium are excited by the electromagnetic wave, which leads to the conversion of a part of the electromagnetic wave energy into kinetic energy. However, there are some works which investigated the path loss of THz signals in blood and tissue, showing that a communication in the range of a few millimeters is feasible [13, 51, 52, 53]. Communication distances of a few millimeters are sufficient for in-body scenarios where large numbers of nanosensors will float inside the blood vessels.

4 Localization approach

As nanosensors are foreseen to float with average velocities of $10 - 20$ cm/s in the bloodstream [54], keeping an updated view of their locations at any point in time is complex in terms of computation and communication costs.
Rather than accurately tracking the highly dynamic nanosensors at any point in time, we propose to add location information to sensor measurements to localize the body regions which show anomalies. Specifically, the nanosensors add IMU information to their actual sensor readings. The system will thus be aware of the body locations at which sensor measurements have been performed. Since nanosensors can only exploit backscattering communication if they are in vicinity of an anchor, anchors implicitly gather information about nanosensor locations whenever they receive a message from a sensor. Figure 5 depicts an overview of the localization system. Nanosensor $s1$ is floating inside the blood vessels while the anchor nodes $a1$ and $a2$ are attached to the skin. Anchors are assumed to constantly transmit RF signals. Whenever a sensor passes by an anchor and receives the RF signal, it exploits the signal to transmit its collected sensor readings along with the IMU readings via backscattering communication to the anchors. Each packet transmitted by a nanosensor includes the ID of the sensor and the actual sensor reading with a location stamp. Whenever a packet was transmitted, nanosensors reset their IMU to the initial state. The reset is done in order to reduce the accumulation error (i.e., the drift) of the IMU.

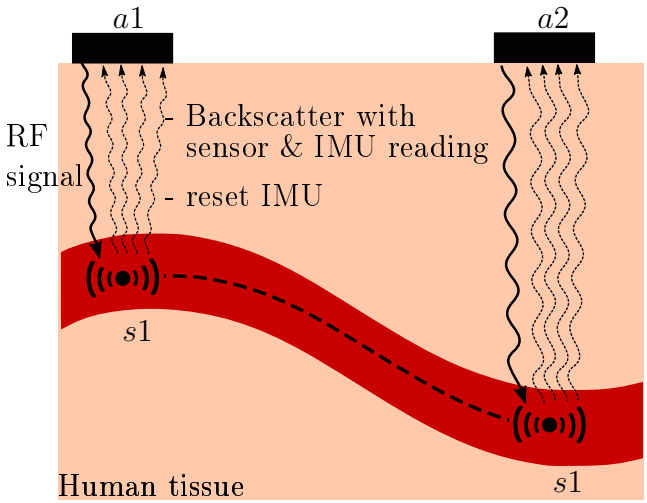

Figure 5: Overview of the proposed localization approach for in-body nanosensors. A nanosensor $s1$ is floating inside a blood vessel. Whenever it is sufficiently close to one of the anchors $a1$ or $a2$, it exploits their RF signal to transmit its sensor reading. After each transmission, the sensor resets its IMU to zero to decrease the accumulation error.

The following subsections discuss the location stamping and the backscattering communication in more detail.

4.1 Location stamping

To be able to provide sensor readings with location stamps, sensors rely on the inertial positioning technique. As discussed in Section 2, inertial positioning refers to the process of estimating a node's current position by using its previous position and an estimate about its traveled distance and direction which are recorded by a built-in IMU.
We propose to equip nanosensors with IMUs including a gyroscope and an accelerometer to be able to measure rotation and velocity and thus get an idea of how far they have traveled within the body. A variety of nanoscale gyroscopes and accelerometers have already been developed in recent years. One example for a nanoscale gyroscope has been presented by Song et al. [55]. The gyroscope has an atom-scale size and is able to provide a sensitivity in the level of 28 rad s^{-1} $Hz^{-1/2}$. Along with gyroscopes, accelerometers based on graphene have been presented as well. One example is the accelerometer proposed by Shi et al. [56] which features a size in the range of tens of μm and a ultra high sensitivity of $8.82 \cdot 10^{-11}$m/m$\cdot s^{-2}$ for a range of $0 - 1000$g. The major drawback of inertial positioning is the accumulation of the error as it

is a recursive process relying on faulty sensor readings. Thus, positions need to be refined (i.e., through sensor fusion) or the IMU needs to be reset whenever possible in order to minimize the error. We thus propose that nanosensors reset their IMU to the initial state whenever they transmit their readings to an anchor. Having a nanosensor communicating to an anchor infers that the sensor is in very close proximity to the anchor, which implicitly gives information about the sensor's current position. The track of the nanosensor packet transmissions thus allows the anchors to keep an updated view of the sensors.

4.2 Backscattering communication

As already mentioned, a promising technique for low-power wireless communication is backscattering communication. Backscattering communication systems consist of two types of devices, a reader (i.e., an anchor) and a tag (i.e., a mobile node) [57]. The tag is the passive component of the system, harvesting energy from an incident RF wave radiated by the reader. Further, the tag modulates and reflects a fraction of the wave back to the reader [57]. Since tags harvest energy from incoming waves, they do not need active RF components while readers are equipped with such. A well known example for a technology which relies on backscattered signals is radio frequency identification (RFID). In the past decade, RFID became a key enabling technology for indoor localization due to its low complexity and energy harvesting capabilities.

In order to be able to modulate the received signal, tags change the antenna reflection properties by varying the impedance of the antenna according to the information they want to communicate. As the antenna load is varied, the reflection coefficients are changed and the reflected signal is modulated [58]. This process is known as backscatter modulation [59] and can achieve different modulation modes including binary pulse amplitude modulation (2-PAM), binary pulse position modulation (2-PPM) and On-Off keying modulation (OOK) [60]. As nanoscale transceivers are not able to generate carrier signals, they need to exploit carrier-less pulse-based communication schemes in any case [45, 28] (refer to Section 3.3).

With their potential of low-power and low heat-radiation wireless communication, backscattering communication tags will most likely be integrated into all kinds of future nanosensor nodes to operate in highly constrained or critical applications including in-body health monitoring.

A backscattering communication channel consists thus of a forward channel from the reader to the tag and a backward channel from the tag to the reader. To model the complete channel and calculate received power and capacity, forward and backward channel need to be taken into account. The backscattered power in dB received at the reader after the signal traveled through the forward and the backward link can

be expressed as [61]

$$P_{R_B}[dB] = P_T + (G_T - L_{tot} + G_R)^2 , \tag{1}$$

where P_T is the transmit power, L_{tot} is the total path loss of the signal and G_T and G_R are the gains of the transmitting and receiving antennas, respectively. The total path loss L_{tot} of the signal mainly depends on the spreading and the molecular absorption loss as the scattering loss can be neglected [62] and is defined as

$$L_{tot}(f) = L_{abs}(f) \times L_{spr}(f) = e^{-\mu_{abs} d} \times \left(\frac{\lambda_g}{4\pi d}\right)^2 , \tag{2}$$

where L_{abs} is the molecular absorption loss, L_{spr} is the spreading loss, μ_{abs} is the molecular absorption coefficient, d is the distance and λ_g is the effective wavelength, which is defined as λ/n'. n' and n'' are the real and imaginary parts of the refractive index n of the medium the wave is travelling through (tissue in our case). The molecular absorption coefficient μ_{abs} depends on the effective wavelength and on the imaginary part of the refractive index and is defines as [13]

$$\mu_{abs} = \frac{4\pi n''}{\lambda_g}. \tag{3}$$

As backscattering reduces the power significantly, also channel capacity is affected. The channel capacity C_B of the forward and the backscattered communication link can be expressed using the Shannon theorem and a flat power distribution as follows:

$$C_B = \sum \Delta f \cdot log_2 \left(1 + \frac{S(f)}{L_{tot}(f,d) N(f,d)}\right), \tag{4}$$

where $S(f)$ is the power spectral density of the signal, Δf is sub-band width, $L_{tot}(f,d)$ is the total loss over the stacked tissue layers (obtained by Equation 2) and $N(f,d)$ is the noise power spectral density. If the sub-band width is small enough, the channel appears as frequency-non selective and the noise power spectral density $S(f)$ can be considered locally flat [50]. According to [63] the noise spectral density can be obtained as

$$N(f,d) = k_B \cdot T_{mol} = k_B \cdot T_0 \left(1 - e^{-4\pi f d n''/c}\right), \tag{5}$$

where k_B is the Boltzmann constant, T_{mol} is the noise temperature due to molecular absorption, T_0 is the reference temperature of 310 K, f is the frequency, d is the distance, c is the speed of light and n'' is the imaginary part of the refractive index of the respective tissue.

5 Evaluation

This section presents systematical evaluation results of the major building blocks of the localization concept. We first discuss the feasibility of in-body THz backscattering communication followed by the restrictions on anchor placement.

5.1 In-body THz backscattering communication

This section investigates the feasibility of THz backscattering communication between nanosensors in the blood and anchors attached to the skin. Further, limited communication distance also implies restrictions on anchor placement which will be discussed. For that purpose we simulate the communication channel to determine path loss and channel capacity. To be able to model the channel, certain biological parameters such as human skin thickness and blood velocity need to be determined. Skin thickness varies a lot across the body and for different bodies. The volar forearm, the scalp, the dorsums of the hand and the anterolateral thigh have average epidermal thicknesses of 90 μm, 108 μm, 181 μm and 60 μm, respectively [64, 65, 66]. The average dermal thicknesses for the aforementioned regions have been measured to be 1100 μm, 1984 μm, 1864 μm and 1950 μm [67, 65, 68]. Based on these measurements, we used simulation values of 200 μm and 1800 μm for epidermal and dermal thickness, respectively. Blood vessels vary a lot in terms of their diameter with $10^{-5}m$ being the smallest in the capillaries, followed by 10^{-4} in the arterioles and 10^{-3} in the small arteries [54]. For our simulation studies, we picked a value of 500 μm for the thickness of the blood layer. The chosen values add up to a total tissue thickness of 2500 μm.

In general, the propagation of THz-band waves inside the human body is drastically impacted by the absorption of liquid water molecules causing internal vibrations into molecules (i.e., absorption loss). The absorption loss is determined using the absorption coefficient of the respective tissue layer. To be able to calculate the absorption coefficient using Equation 3, the dielectric characteristics of the tissue layers are required. Table 1 summarizes the dielectric parameters of epidermis, dermis and blood which were used in our simulations.

Figure 6 shows the absorption coefficient of the different human tissue layers at sub-THz frequencies. As we can see from the figure, the absorption loss is more dominant in blood than in the other tissue layers, which is due to the fact that blood contains the highest amount of water molecules.

Using the absorption coefficient μ_{abs} and the equations for spreading and absorption loss (see Equation 2), we determined the spreading and the absorption loss for the three tissue layers. Figure 7 shows the spreading loss (a) and the absorption loss (b) in dB at 0.5 THz for the blood, dermis and epidermis over increasing distance. As can be seen from the figures, the signal suffers significantly more from molecular

Table 1: Permittivity and relaxation time values for blood, dermis and epidermis.

Parameter	Blood	Dermis	Epidermis
α_1		0.92	0.95
α_2		0.97	
β_1		0.8	0.96
β_2		0.99	
ε_∞	2.1	4	3.0
ε_1	130	5.96	89.61
ε_2	3.8	380.4	
τ_1 (ps)	14.4	1.6	15.9
τ_2 (ps)	0.1	159 (ns)	
σ		0.1	
Ref.	[69]	[51]	[51]

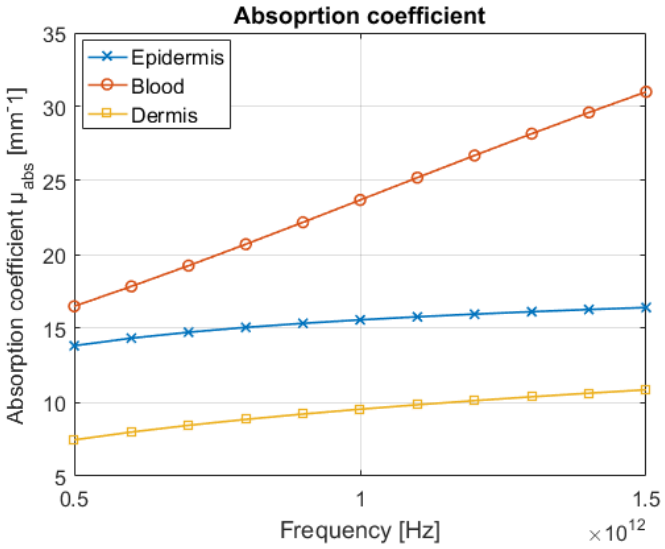

Figure 6: Absorption coefficient μ_{abs} of epidermis, dermis and blood in the sub-terahertz band.

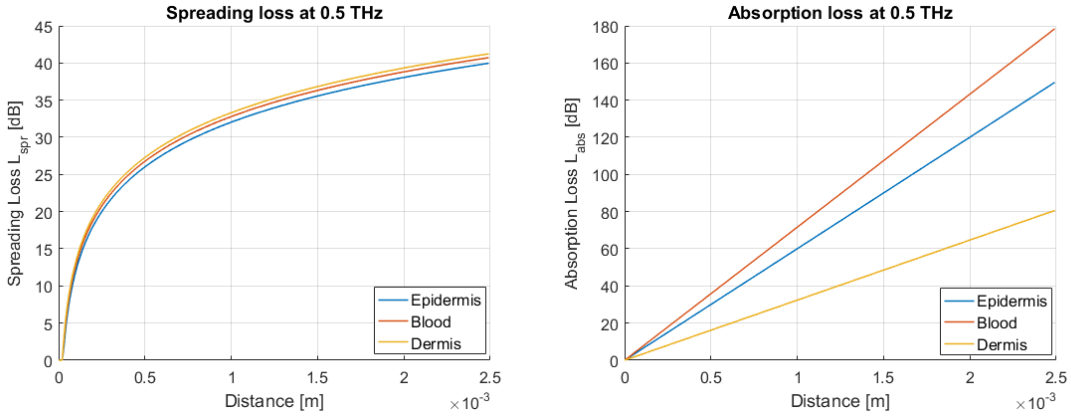

(a) a (b) b

Figure 7: Spreading (a) and absorption loss (b) at 0.5 THz for the different human tissue layers over distance.

absorption than from spreading loss.

Since we propose to rely on backscattering communication, we are specifically interested in the backscattered power received at the anchor and defined by Equation 1. Therefore, we connected the tissue layers into a stack and modeled a signal traveling the channel twice (from the anchor to the nanosensor and back). The thicknesses of the layers were thereby chosen as discussed above and the antenna gains G_T and G_R were chosen to be 5.09 [70]. In line with [51, 50], the pulse energy and the pulse duration are assumed to be constant at 500 pJ and 100 fs, resulting in a transmitted peak power of 5 kW.

Figure 8 shows the received backscattered power P_{R_B} in dB for frequencies of $0.5, 0.8$ and 1 THz over the three layers after being transmitted through 500 μm of blood, 1800 μm of dermis and 200 μm of epidermis (adding up to a total distance of 2500 μm). As can be seen from the figure, after traveling twice through blood, dermis and epidermis, the signal power received at the anchor is approx. -156, -185 and -198 dB depending on the used frequency.

Receiving a signal at -156 dB requires the receiver to have a sensitivity of approx. 0.25 fW/Hz$^{1/2}$. The requirement for the sensitivity can be eased by applying a higher transmit power or by using higher gain antennas. Nonetheless, nanoelectronic detectors with sensitivities of 10^{-15} - 10^{-20} W/Hz$^{1/2}$ have already been proposed in literature [71, 72, 73, 74].

The state-of-the-art further shows that channel capacities on the order of Gbps-Tbps can be achieved for distances below 4 mm in in-body THz communication scenarios [51, 75, 53]. As backscattering reduces the power significantly, also channel capacity is affected. We calculated the channel capacity C_B of the forward and the backscat-

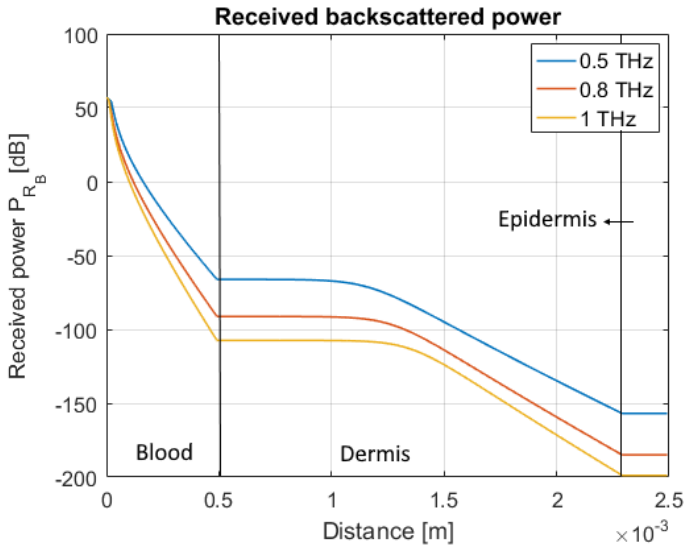

Figure 8: Received backscattered power P_{R_B} in dB for frequencies of $0.5, 0.8$ and 1 THz over a distance of 2500 μm and three stacked tissue layers.

tered communication link using Equation 4. We used the initial transmission power of the anchor to determine $S(f)$ for the forward link, and the power received at the nanosensor to determine $S(f)$ for the backscattered link.
Figure 9 shows the theoretical capacity of the forward (a) and the backscattered (b) communication link for the stacked tissue layers. In line with the related work [51, 75, 53], the capacity for the forward link at a distance of 2500μm is in the order of Tbps. However, the capacity of the backscattered link is drastically decreased to approx. 1 kbps. To be able to achieve higher capacities in backscattering communication, the system will require significantly higher transmit power and/or antenna gains. Generally speaking, channel capacities on the order of kbps are more realistically achievable than Gbps.
Summarized, sub-THz backscattering communication in human tissue is feasible for very limited distances. Specifically, the anchors should be attached to regions of the body where the skin and fat layers are thin, i.e., volar forearm, scalp or dorsum of the hand.

5.2 Anchor placement

This section studies the movement of the nanosensors in the bloodstream and the amount of anchors required to establish a stable in-body localization and communication system with reasonable positioning error. We specifically explore movement and message volume of nanosensors to get an idea about how close anchors need to

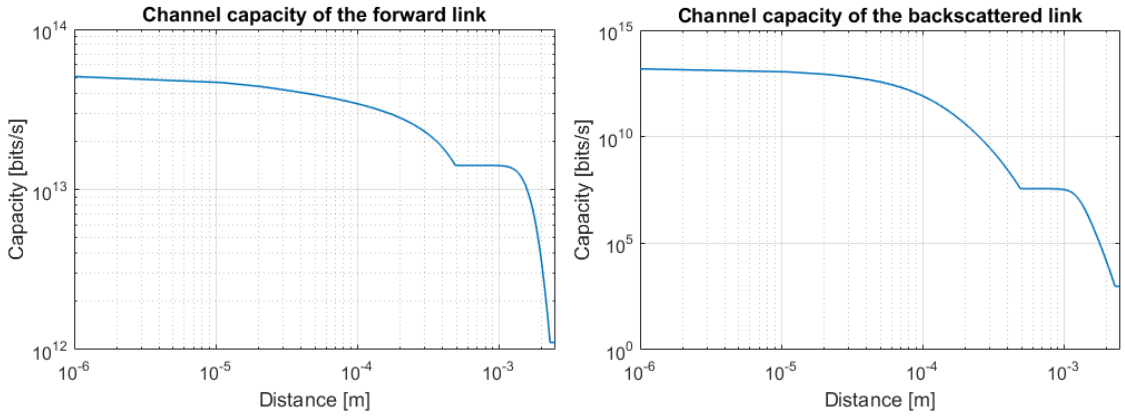

(a) a (b) b

Figure 9: Channel capacity of the forward link (a) and the backscattered link (b) for the stacked human tissue layers and a total distance of 2500μm.

be placed to each other such that the system is capable of coping with a localization error and minimizing the on-board storage and communication bandwidth requirements.
The following three factors mainly influence the placement of anchors: i.) limited distance between sensors and anchors due to the THz backscattering communication, ii.) the limited resources in terms of on-board sensor storage and communication bandwidth and iii.) the accumulated localization error due to the IMU drift over time. The maximum achievable communication distance has already been discussed in the previous section. Regarding the limited resources, we discuss the message format and amount of sensor readings which need to be stored and transmitted by nanosensors. The results will show that the limited resources require anchors to be place quite close to each other, which in turn eases the requirements on IMU accuracy.

Limited resources Nanosensors are foreseen to collect sensor readings along with IMU measurements until they pass by an anchor and are able to transmit all the readings and reset the IMU to its initial state. As sensors are equipped with a processor, they are assumed to be capable of determining locations from the IMU readings on-board. Figure 2 shows the format of a sensor message, which includes the sensor's ID, the actual sensor reading which is of interest for the respective health monitoring application (i.e., pressure, temperature) and the gyroscope and accelerometer readings obtained simultaneously with the sensor reading.
Assuming the ID to be an integer value and all other readings to be double values, the message payload requires a size of $32 + 7 \cdot 64 = 448$ bits. Even if the theoretical

Sensor ID	Sensor reading	Gyro X	Gyro Y	Gyro Z	Acc X	Acc Y	Acc Z
32bit	64bit	64bit	64bit	64bit	64bit	64bit	64bit

Table 2: Message format.

capacity of 1 kbps (see Figure 9) may not be fully achieved, there is still space for headers and bit error correction codes along with the message payload. For each sensor reading, a nanosensor thus requires $448/8 = 56$ byte of memory to store it until floating by an anchor such that it can be transmitted. One of the smallest (50 nm), fastest (sub−5 ns) and thinnest (8 nm) graphene oxide based memory devices was introduced in 2017 and enables multilevel (4−level, 2−bit per cell) storage capabilities [76]. If we assume that the in-body nanosensor has a size of 5×5 μm^2, it would be able to fit 10 000 memory cells, each able to store 2 bit. In total, such a nanomemory would thus be able to store 20 000 bits corresponding to 2500 byte. Theoretically, such a nanomemory could thus store approx. 44 messages of the above mentioned message format. Naturally, storage capabilities are directly affected by the size of the nanosensor.
Not only memory but also communication bandwidth is a limiting factor when it comes to the amount of sensor messages that can be transferred at once from a nanosensor to an anchor. A channel capacity of 1 kbps means that 1000 bits can be transmitted per second in the best case (i.e., good link quality, low noise). Assuming anchor nodes have a size of about 5×5 cm^2, nanosensors would need 0.25 s in the aorta, 0.5 s in the arteries and 1.7 s in the veins to pass by an anchor. This consideration suggests that nanosensors cannot transmit more than two messages to an anchor while floating by.

Simulation Modeling all characteristics of the cardiovascular system is non-trivial as it comprises approx. 4900 cm^3 of blood volume and 120 000 km of blood vessels [77]. The blood flow rate depends on the diameter of the vessel reaching from $10-20$ cm/s in the arteries over 0.1 cm/s in the arterioles to $5 \cdot 10^{-3}$ cm/s in the capillaries [54]. There is no simulation tool available yet, which incorporates the entire circulatory system in detail. However, to be able to achieve estimates about the required amount of anchors for our localization system, a simplified model including all major vessels of the cardiovascular system is sufficient. Therefore, we used BloodVoyagerS [78], which is a medical nanonetwork simulation module for ns-3[1]. BloodVoyagerS is modeled upon a simplified human cardiovascular system to realize the movement of nanobots within the human bloodstream. The simulator comprises a model including 94 vessels and their respective blood flow rates (20 cm/s in the aorta, 10 cm/s in the arteries, $2-4$ cm/s in the veins), adding up to a total simulated vessel

[1] https://www.nsnam.org/

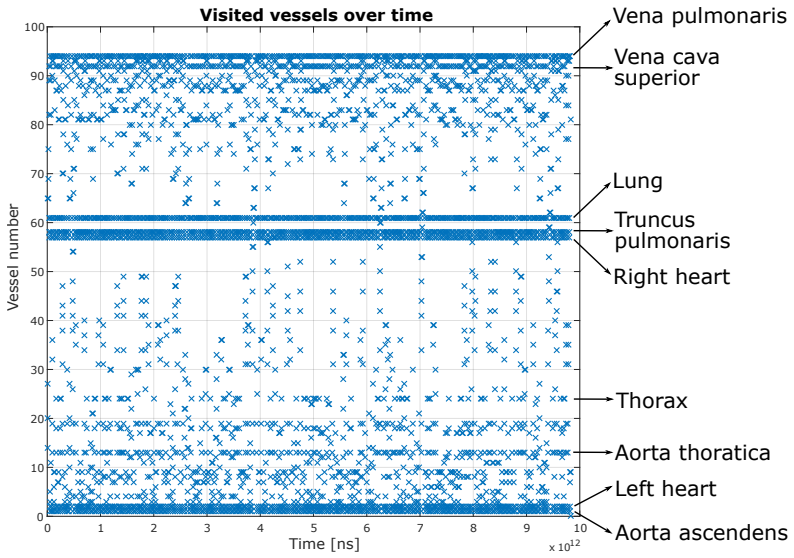

Figure 10: Visited vessels over time.

length of 12 717 m (based on measurements of a person with 1.72 m height and 69 kg weight).
Using this simulator, we evaluated how often nanosensors pass by an anchor when floating in the bloodstream. Therefore we simulated two different anchor setups and relied on the blood flow model of the simulation tool. Knowing how frequently nanosensors pass by anchors also allows us to provide estimates on required accuracy of future nano-IMUs. In a first step, we were interested in the movement of the nanosensors, in order to get an idea which body locations are visited the most. For that purpose, we performed a simulation of one nanosensor moving in the cardiovascular system for 10 000 s. Figure 10 shows which vessels have been visited by the nanosensor at each timestep. In BloodVoyagerS, all vessels and organs have a dedicated number. The x-axis of Figure 10 shows the numbers of the respective vessel (refer to [78] for all vessel numbers) and the y-axis shows the timestep in ns. We annotated the most visited vessels to show which body locations are reached more frequently than others. As expected, the nanosensor passes more often through upper body regions like the heart and the lungs than the extremities. This results suggests to place more anchors around the upper body to have nanosensors floating by anchors more often.

In a next step, we simulated two different anchor setups, one including 20 anchors and the other 30. The locations were chosen such that anchors are well distributed across the body.
To study how often a sensor would pass by an anchor in these two setups, we injected one nanosensor into the brachial artery (upper left arm) and tracked its movement

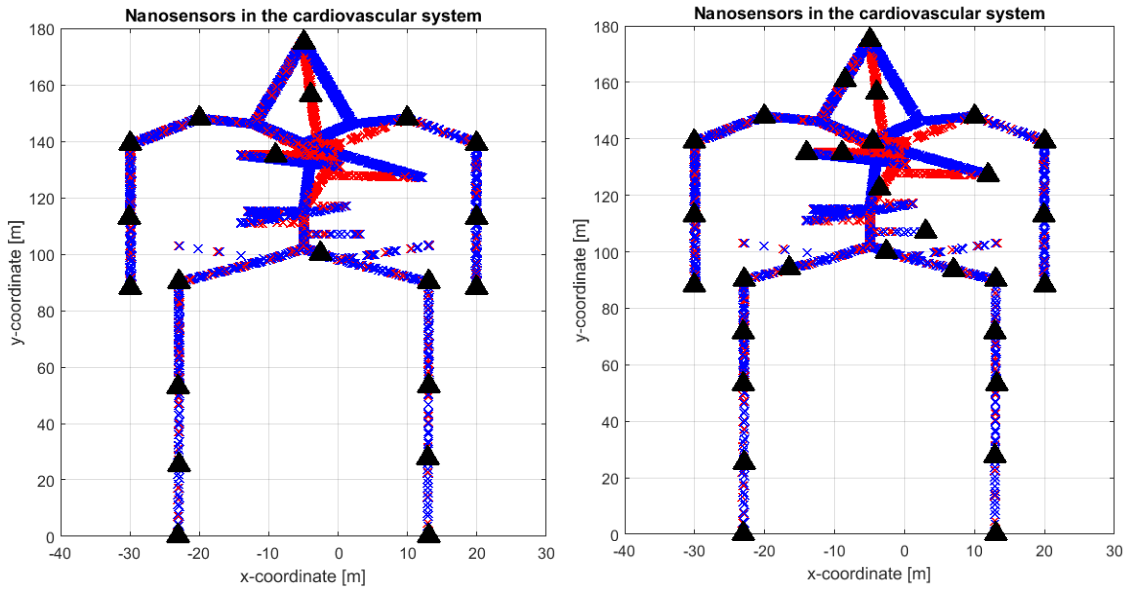

(a) a (b) b

Figure 11: Simulation results of one nanosensor moving through the cardiovascular system for 10 000 s for a setup of (a) 20 and (b) 30 anchors. Red and blue crosses depict the location of the nanosensor, whereby red indicates arteries and blue indicates veins. The black triangles depict the anchor locations.

for 10 000 s (approx. 2.7 h). We ran the simulation 50 times and averaged the results to determine how often the nanosensor has floated by an anchor. Figure 11 shows the simulation results for the (a) 20 and (b) 30 anchor setup in terms of nanosensor locations (x and y) recorded over time and depicted by red (artery) and blue (vein) crosses. The black triangles depict the anchor locations. Using the track of the nanosensor, we determined each timestep at which the sensor was in close proximity to an anchor (i.e., the nanosensor is within a 5 cm radius of an anchor). Figure 12 shows the probability distribution of the duration between two anchor visits for the (a) 20 and (b) 30 anchor setup. In both cases, almost 80% of consecutive anchor visits occurred within a time window of 10 s (first bar in each histogram). As expected, the probability of shorter durations between anchor visits is higher for the 30 anchor setup. Specifically, in the 20 anchors setup, a visit might take up to 80 s in the worst case, while its only 40 s in the 30 anchors setup. Based on these results, we consider the 30 anchors setup as more realistic since it ensures that most of the anchors visits occur within 20 s. Considering that 80% of the time anchor visits occur within 10 s, an appropriate sampling rate for acquiring sensor readings could be chosen as $0.1 - 0.2$ Hz (sensor measurements are performed every $5 - 10$ s. The sampling rate depends on the requirements of the application, however, sampling

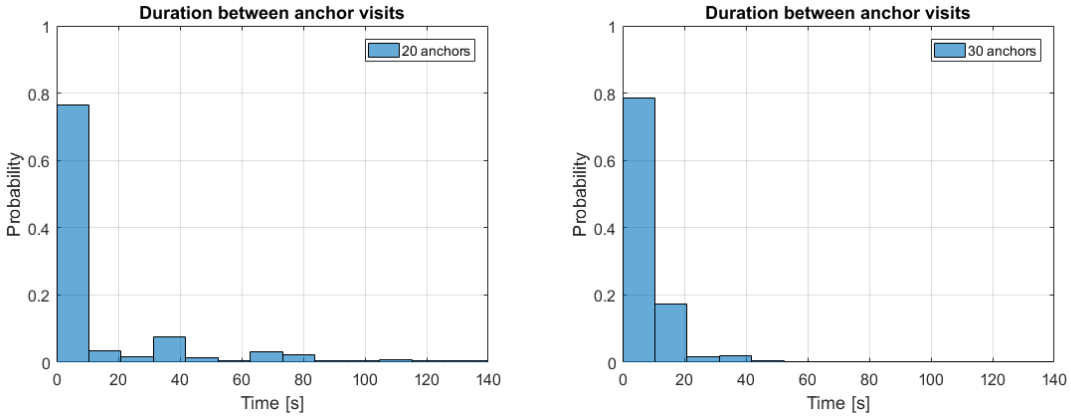

(a) a (b) b

Figure 12: Probability distributions of the durations between two anchor visits for the (a) 20 and (b) 30 anchor setup.

rates of up to 4 Hz are realistically achievable for current nanosensor prototypes [37, 39].
If anchors are placed approx. 20 cm apart from each other (as in the 30 anchor setup), nanosensors are able to frequently transmit their sensor readings and thus reset their IMUs. Therefore, the requirements on IMU accuracy are not very strict. Furthermore, anchors will implicitly get a good overview of the nanosensor locations as they float by. A localization approach based on IMU measurements implies that the monitored person does not move, which we consider as moderate requirement for medical applications.

6 Conclusion

Traditional localization technologies are not feasible for in-body scenarios due to the specific communication and resource constraints of nanosensors as well as the highly dynamic environment. This work proposes a novel localization concept for nanosensors floating in the human bloodstream. The outlined system comprises nanosensors as well as anchor nodes attached to the human skin, and relies on inertial positioning and THz backscattering communication. Simulations have been performed as a proof of concept and provide promising results. As nanosensors are still in the development process, our approach can be seen as a starting point for the development of localization methods for future health monitoring applications. To further improve our concept, future work should specifically be investigated with an interdisciplinary team to explore the feasibility of nanosensors (with built-in IMUs) and human health and safety considerations.

7 Dissemination

This work has been disseminated in two ways. We submitted an abstract to the Austrian Research and Innovation Talk (ARIT)[2] which is organized by the Office of Science and Technology Austria (OSTA) in Washington D.C. Our abstract was ranked among the top ten submission, which makes us eligible for competing for this year's poster award. The poster and a 1-minute video pitch, which we prepared for the competition, can be found online [3]. The poster award winners will be announced at on September 17th at the ARIT, which will take place virtually this year. Through my top ten ranking at the ARIT, I also became a member of the Austrian Research and Innovation Network[4] (RINA), which enables me to connect with a large network of Austrian researchers.
Furthermore, we almost finished the journal paper writing and will submit it to IEEE Transactions on NanoBioscience within the coming weeks.

[2]https://www.ostaustria.org/arit-2020
[3]https://www.ostaustria.org/arit-2020-poster-session-voting-platform
[4]https://www.ostaustria.org/rina

References

[1] T. Panigrahi, M. Hassan *et al.*, "Energy efficient event localization and classification for nano iot," in *Proceedings of the IEEE Global Communications Conference (GLOBECOM)*. IEEE, 2018, pp. 1–6.

[2] J. M. Jornet and I. F. Akyildiz, "The internet of multimedia nano-things," *Nano Communication Networks*, vol. 3, no. 4, pp. 242–251, 2012.

[3] J. Simonjan, J. M. Jornet, I. F. Akyildiz, and B. Rinner, "Nano-cameras: a key enabling technology for the internet of multimedia nano-things," in *Proceedings of the 5th ACM International Conference on Nanoscale Computing and Communication*, 2018, pp. 1–6.

[4] F. D. Natterer, K. Yang, W. Paul, P. Willke, T. Choi, T. Greber, A. J. Heinrich, and C. P. Lutz, "Reading and writing single-atom magnets," *Nature*, vol. 543, no. 7644, p. 226, 2017.

[5] Y. V. Gerasimova and D. M. Kolpashchikov, "Towards a dna nanoprocessor: Reusable tile-integrated dna circuits," *Angewandte Chemie*, vol. 128, no. 35, pp. 10 400–10 403, 2016.

[6] I. F. Akyildiz and J. M. Jornet, "Electromagnetic wireless nanosensor networks," *Nano Communication Networks*, vol. 1, no. 1, pp. 3–19, 2010.

[7] L. Ji, P. Meduri, V. Agubra, X. Xiao, and M. Alcoutlabi, "Graphene-based nanocomposites for energy storage," *Advanced Energy Materials*, vol. 6, no. 16, 2016.

[8] F. R. Fan, W. Tang, and Z. L. Wang, "Flexible nanogenerators for energy harvesting and self-powered electronics," *Advanced Materials*, vol. 28, no. 22, pp. 4283–4305, 2016.

[9] H. Chen, H. Liu, Z. Zhang, K. Hu, and X. Fang, "Nanostructured photodetectors: from ultraviolet to terahertz," *Advanced Materials*, vol. 28, no. 3, pp. 403–433, 2016.

[10] P. Singh and R. Yadava, "Nanosensors for health care," in *Nanosensors for Smart Cities*. Elsevier, 2020, pp. 433–450.

[11] A. Munawar, Y. Ong, R. Schirhagl, M. A. Tahir, W. S. Khan, and S. Z. Bajwa, "Nanosensors for diagnosis with optical, electric and mechanical transducers," *RSC advances*, vol. 9, no. 12, pp. 6793–6803, 2019.

[12] J. M. Jornet and I. F. Akyildiz, "Graphene-based plasmonic nano-antenna for terahertz band communication in nanonetworks," *IEEE Journal on selected areas in communications*, vol. 31, no. 12, pp. 685–694, 2013.

[13] H. Elayan, R. M. Shubair, J. M. Jornet, and P. Johari, "Terahertz channel model and link budget analysis for intrabody nanoscale communication," *IEEE transactions on nanobioscience*, vol. 16, no. 6, pp. 491–503, 2017.

[14] J. Simonjan and B. Rinner, "Decentralized and resource-efficient self-calibration of visual sensor networks," *Ad Hoc Networks*, vol. 88, pp. 112 – 128, 2019.

[15] N. A. Alrajeh, M. Bashir, and B. Shams, "Localization techniques in wireless sensor networks," *International Journal of Distributed Sensor Networks*, vol. 9, no. 6, 2013, Article ID 304628.

[16] C. Li, S. Wang, Y. Zhuang, and F. Yan, "Deep sensor fusion between 2d laser scanner and imu for mobile robot localization," *IEEE Sensors Journal*, 2019.

[17] T. He, C. Huang, B. M. Blum, J. A. Stankovic, and T. F. Abdelzaher, "Range-free localization and its impact on large scale sensor networks," *ACM Transactions on Embedded Computing Systems (TECS)*, vol. 4, no. 4, pp. 877–906, 2005.

[18] P. Rong and M. L. Sichitiu, "Angle of arrival localization for wireless sensor networks," in *Proceedings of the Third Annual IEEE Communications Society on Sensor and Ad Hoc Communications and Networks*, vol. 1. IEEE, 2006, pp. 374–382.

[19] I. T. Haque and C. Assi, "Profiling-based indoor localization schemes," *IEEE Systems Journal*, vol. 9, no. 1, pp. 76–85, 2015.

[20] D. Niculescu and B. Nath, "Ad hoc positioning system (aps)," in *IEEE Global Telecommunications Conference (GLOBECOM)*, vol. 5. IEEE, 2001, pp. 2926–2931.

[21] G. Mao, B. Fidan, and B. D. Anderson, "Wireless sensor network localization techniques," *Computer Networks*, vol. 51, no. 10, pp. 2529–2553, 2007.

[22] K. Stone and T. Camp, "A survey of distance-based wireless sensor network localization techniques," *International Journal of Pervasive Computing and Communications*, vol. 8, no. 2, pp. 158–183, 2012.

[23] L. Zhou, G. Han, and L. Liu, "Pulse-based distance accumulation localization algorithm for wireless nanosensor networks," *IEEE Access*, vol. 5, pp. 14 380–14 390, 2017.

[24] A. Awad, T. Frunzke, and F. Dressler, "Adaptive distance estimation and localization in wsn using rssi measures," in *Proceedings of the 10th Euromicro Conference on Digital System Design Architectures, Methods and Tools*. IEEE, 2007, pp. 471–478.

[25] J. M. Barcelo-Ordinas, M. Doudou, J. Garcia-Vidal, and N. Badache, "Self-calibration methods for uncontrolled environments in sensor networks: A reference survey," *Ad Hoc Networks*, vol. 88, pp. 142–159, 2019.

[26] F. Lemic, S. Abadal, W. Tavernier, P. Stroobant, D. Colle, E. Alarcón, J. Marquez-Barja, and J. Famaey, "Survey on terahertz nanocommunication and networking: A top-down perspective," *arXiv preprint arXiv:1909.05703*, 2019.

[27] H. Tran-Dang, N. Krommenacker, and P. Charpentier, "Localization algorithms based on hop counting for wireless nano-sensor networks," in *2014 International Conference on Indoor Positioning and Indoor Navigation (IPIN)*. IEEE, 2014, pp. 300–306.

[28] M. S. Prasad, T. Panigrahi, and M. Hassan, "Direction of arrival estimation for nanoscale sensor networks," in *Proceedings of the 5th ACM International Conference on Nanoscale Computing and Communication*. ACM, 2018, p. 21.

[29] P. Stoica and A. Nehorai, "Music, maximum likelihood, and cramer-rao bound," *IEEE Transactions on Acoustics, speech, and signal processing*, vol. 37, no. 5, pp. 720–741, 1989.

[30] M. El-Absi, A. A. Abbas, A. Abuelhaija, F. Zheng, K. Solbach, and T. Kaiser, "High-accuracy indoor localization based on chipless rfid systems at thz band," *IEEE Access*, vol. 6, pp. 54 355–54 368, 2018.

[31] F. Lemic, S. Abadal, and J. Famaey, "Toward localization in terahertz-operating energy harvesting software-defined metamaterials: Context analysis," in *Proceedings of the Seventh Annual International Conference on Nanoscale Computing and Communication (NANOCOM)*. ACM, 2020, [to appear].

[32] H. Sarieddeen, N. Saeed, T. Y. Al-Naffouri, and M.-S. Alouini, "Next generation terahertz communications: A rendezvous of sensing, imaging, and localization," *IEEE Communications Magazine*, vol. 58, no. 5, pp. 69–75, 2020.

[33] A. Marquez, B. Tank, S. K. Meghani, S. Ahmed, and K. Tepe, "Accurate uwb and imu based indoor localization for autonomous robots," in *Proceedings of the 30th Canadian Conference on Electrical and Computer Engineering (CCECE)*. IEEE, 2017, pp. 1–4.

[34] V. Malyavej, W. Kumkeaw, and M. Aorpimai, "Indoor robot localization by rssi/imu sensor fusion," in *Proceedings of the 10th International Conference on Electrical Engineering/Electronics, Computer, Telecommunications and Information Technology*. IEEE, 2013, pp. 1–6.

[35] T. Khan, M. Civas, O. Cetinkaya, N. A. Abbasi, and O. B. Akan, "Nanosensor networks for smart health care," in *Nanosensors for Smart Cities*. Elsevier, 2020, pp. 387–403.

[36] I. Santiago, "Nanoscale active matter matters: Challenges and opportunities for self-propelled nanomotors," *Nano Today*, vol. 19, pp. 11–15, 2018.

[37] H. Li, K. Wu, Z. Xu, Z. Wang, Y. Meng, and L. Li, "Ultrahigh-sensitivity piezoresistive pressure sensors for detection of tiny pressure," *ACS applied materials & interfaces*, vol. 10, no. 24, pp. 20 826–20 834, 2018.

[38] R. Rajasekar and S. Robinson, "Nano-pressure and temperature sensor based on hexagonal photonic crystal ring resonator," *Plasmonics*, vol. 14, no. 1, pp. 3–15, 2019.

[39] Z. Qu, L. Wu, B. Yue, Y. An, Z. Liu, P. Zhao, J. Luo, Y. Xie, Y. Liu, Q. Wang *et al.*, "Eccentric triboelectric nanosensor for monitoring mechanical movements," *Nano Energy*, vol. 62, pp. 348–354, 2019.

[40] M. E. Tanner and J. M. Protz, "The feasibility of a nano-interial measurement unit that uses chemistry to record position," in *Chemical and Biological Sensing VIII*, vol. 6554. International Society for Optics and Photonics, 2007, p. 65540H.

[41] J. W. Kang, J. H. Lee, H. J. Hwang, and K.-S. Kim, "Developing accelerometer based on graphene nanoribbon resonators," *Physics Letters A*, vol. 376, no. 45, pp. 3248–3255, 2012.

[42] Z. Yang, M. Nakajima, Y. Shen, and T. Fukuda, "Nano-gyroscope assembly using carbon nanotube based on nanorobotic manipulation," in *Proceedings of the International Symposium on Micro-NanoMechatronics and Human Science*. IEEE, 2011, pp. 309–314.

[43] M. Ahmadian, K. Jafari, and M. J. Sharifi, "Novel graphene-based optical mems accelerometer dependent on intensity modulation," *ETRI Journal*, vol. 40, no. 6, pp. 794–801, 2018.

[44] T. Kürner and S. Priebe, "Towards thz communications-status in research, standardization and regulation," *Journal of Infrared, Millimeter, and Terahertz Waves*, vol. 35, no. 1, pp. 53–62, 2014.

[45] J. M. Jornet and I. F. Akyildiz, "Femtosecond-long pulse-based modulation for terahertz band communication in nanonetworks," *IEEE Transactions on Communications*, vol. 62, no. 5, pp. 1742–1754, 2014.

[46] A. P. Shrestha, S.-J. Yoo, H. J. Choi, and K. S. Kwak, "Enhanced rate division multiple access for electromagnetic nanonetworks," *IEEE Sensors Journal*, vol. 16, no. 19, pp. 7287–7296, 2016.

[47] H. Mabed and J. Bourgeois, "A flexible medium access control protocol for dense terahertz nanonetworks," in *Proceedings of the 5th ACM International Conference on Nanoscale Computing and Communication*, 2018, pp. 1–7.

[48] A. K. Vavouris, F. D. Dervisi, V. K. Papanikolaou, and G. K. Karagiannidis, "An energy efficient modulation scheme for body-centric nano-communications in the thz band," in *Proceedings of the 7th International Conference on Modern Circuits and Systems Technologies (MOCAST)*. IEEE, 2018, pp. 1–4.

[49] J. Kokkoniemi, J. Lehtomäki, and M. Juntti, "A discussion on molecular absorption noise in the terahertz band," *Nano Communication Networks*, vol. 8, pp. 35 – 45, 2016, electromagnetic Communication in Nanoscale. [Online]. Available: http://www.sciencedirect.com/science/article/pii/S1878778915000472

[50] J. M. Jornet and I. F. Akyildiz, "Channel modeling and capacity analysis for electromagnetic wireless nanonetworks in the terahertz band," *IEEE Transactions on Wireless Communications*, vol. 10, no. 10, pp. 3211–3221, 2011.

[51] G. Piro, P. Bia, G. Boggia, D. Caratelli, L. A. Grieco, and L. Mescia, "Terahertz electromagnetic field propagation in human tissues: A study on communication capabilities," *Nano Communication Networks*, vol. 10, pp. 51–59, 2016.

[52] N. Chopra, K. Yang, Q. H. Abbasi, K. A. Qaraqe, M. Philpott, and A. Alomainy, "Thz time-domain spectroscopy of human skin tissue for in-body nanonetworks," *IEEE Transactions on Terahertz Science and Technology*, vol. 6, no. 6, pp. 803–809, 2016.

[53] G. Piro, K. Yang, G. Boggia, N. Chopra, L. A. Grieco, and A. Alomainy, "Terahertz communications in human tissues at the nanoscale for healthcare applications," *IEEE Transactions on Nanotechnology*, vol. 14, no. 3, pp. 404–406, 2015.

[54] M. Fruchard, L. Arcese, and E. Courtial, "Estimation of the blood velocity for nanorobotics," *IEEE Transactions on Robotics*, vol. 30, no. 1, pp. 93–102, 2013.

[55] X. Song, L. Wang, F. Feng, L. Lou, W. Diao, and C. Duan, "Nanoscale quantum gyroscope using a single 13c nuclear spin coupled with a nearby nv center in diamond," *Journal of Applied Physics*, vol. 123, no. 11, p. 114301, 2018.

[56] F.-T. Shi, S.-C. Fan, C. Li, and X.-B. Peng, "Modeling and analysis of a novel ultrasensitive differential resonant graphene micro-accelerometer with wide measurement range," *Sensors*, vol. 18, no. 7, p. 2266, 2018.

[57] W. Liu, K. Huang, X. Zhou, and S. Durrani, "Next generation backscatter communication: systems, techniques, and applications," *EURASIP Journal on Wireless Communications and Networking*, vol. 2019, no. 1, pp. 1–11, 2019.

[58] S. Khaledian, F. Farzami, H. Soury, B. Smida, and D. Erricolo, "Active two-way backscatter modulation: An analytical study," *IEEE Transactions on Wireless Communications*, vol. 18, no. 3, pp. 1874–1886, 2019.

[59] D. Dardari, F. Guidi, C. Roblin, and A. Sibille, "Ultra-wide bandwidth backscatter modulation: Processing schemes and performance," *EURASIP Journal on Wireless Communications and Networking*, vol. 2011, no. 1, p. 47, 2011.

[60] D. Dardari, "Method and apparatus for communication in ultra-wide bandwidth rfid systems," 2015, uS Patent 8,952,789.

[61] J. D. Griffin and G. D. Durgin, "Complete link budgets for backscatter-radio and rfid systems," *IEEE Antennas and Propagation Magazine*, vol. 51, no. 2, pp. 11–25, 2009.

[62] H. Elayan, R. M. Shubair, J. M. Jornet, and R. Mittra, "Multi-layer intrabody terahertz wave propagation model for nanobiosensing applications," *Nano communication networks*, vol. 14, pp. 9–15, 2017.

[63] K. Yang, A. Pellegrini, M. O. Munoz, A. Brizzi, A. Alomainy, and Y. Hao, "Numerical analysis and characterization of thz propagation channel for body-centric nano-communications," *IEEE Transactions on Terahertz Science and technology*, vol. 5, no. 3, pp. 419–426, 2015.

[64] R. Maiti, L.-C. Gerhardt, Z. S. Lee, R. A. Byers, D. Woods, J. A. Sanz-Herrera, S. E. Franklin, R. Lewis, S. J. Matcher, and M. J. Carré, "In vivo measurement of skin surface strain and sub-surface layer deformation induced by natural tissue stretching," *Journal of the Mechanical Behavior of Biomedical Materials*, vol. 62, pp. 556–569, 2016.

[65] P. Oltulu, B. Ince, N. Kökbudak, F. Kılıç *et al.*, "Measurement of epidermis, dermis, and total skin thicknesses from six different body regions with a new ethical histometric technique," *Türk Plastik, Rekonstrüktif ve Estetik Cerrahi Dergisi (Turk J Plast Surg)*, vol. 26, no. 2, pp. 56–61, 2018.

[66] J. C. Chan, J. Ward, F. Quondamatteo, P. Dockery, and J. L. Kelly, "Skin thickness of the anterior, anteromedial, and anterolateral thigh: A cadaveric study for split-skin graft donor sites," *Archives of plastic surgery*, vol. 41, no. 6, p. 673, 2014.

[67] F. Hendriks, D. Brokken, C. Oomens, F. Baaijens, and F. Morales-Serrano, "Characterization of mechanical properties of human dermis in vivo," in *Mate Poster Award 2002: 7th Annual Poster Contest*, 2002.

[68] O. Akkus, A. Oguz, M. Uzunlulu, M. Kizilgul *et al.*, "Evaluation of skin and subcutaneous adipose tissue thickness for optimal insulin injection," *J Diabetes Metab*, vol. 3, no. 8, p. 2, 2012.

[69] C. B. Reid, G. Reese, A. P. Gibson, and V. P. Wallace, "Terahertz time-domain spectroscopy of human blood," *IEEE journal of biomedical and health informatics*, vol. 17, no. 4, pp. 774–778, 2013.

[70] M. M. Seyedsharbaty and R. A. Sadeghzadeh, "Antenna gain enhancement by using metamaterial radome at thz band with reconfigurable characteristics based on graphene load," *Optical and Quantum Electronics*, vol. 49, no. 6, p. 221, 2017.

[71] A. Rogalski, *Infrared and Terahertz Detectors*. CRC Press, 2019.

[72] ——, "Terahertz detectors," *Encyclopedia of Modern Optics*, p. 418, 2018.

[73] A. Rogalski, M. Kopytko, and P. Martyniuk, "Two-dimensional infrared and terahertz detectors: Outlook and status," *Applied Physics Reviews*, vol. 6, no. 2, p. 021316, 2019.

[74] H. Ito and T. Ishibashi, "Highly sensitive terahertz-wave detection by fermi-level managed barrier diode," in *Optical Sensing, Imaging, and Photon Counting: From X-Rays to THz*, vol. 11088. International Society for Optics and Photonics, 2019, p. 1108807.

[75] S. F. Bush, J. L. Paluh, G. Piro, V. Rao, R. V. Prasad, and A. Eckford, "Defining communication at the bottom," *IEEE Transactions on Molecular, Biological and Multi-Scale Communications*, vol. 1, no. 1, pp. 90–96, 2015.

[76] V. K. Nagareddy, M. D. Barnes, F. Zipoli, K. T. Lai, A. M. Alexeev, M. F. Craciun, and C. D. Wright, "Multilevel ultrafast flexible nanoscale nonvolatile hybrid graphene oxide–titanium oxide memories," *ACS nano*, vol. 11, no. 3, pp. 3010–3021, 2017.

[77] G. J. Tortora and B. H. Derrickson, *Principles of anatomy and physiology*. John Wiley & Sons, 2018.

[78] R. Geyer, M. Stelzner, F. Büther, and S. Ebers, "Bloodvoyagers: simulation of the work environment of medical nanobots," in *Proceedings of the 5th ACM International Conference on Nanoscale Computing and Communication*, 2018, pp. 1–6.